Volume 1 | Number 1 | January 2017

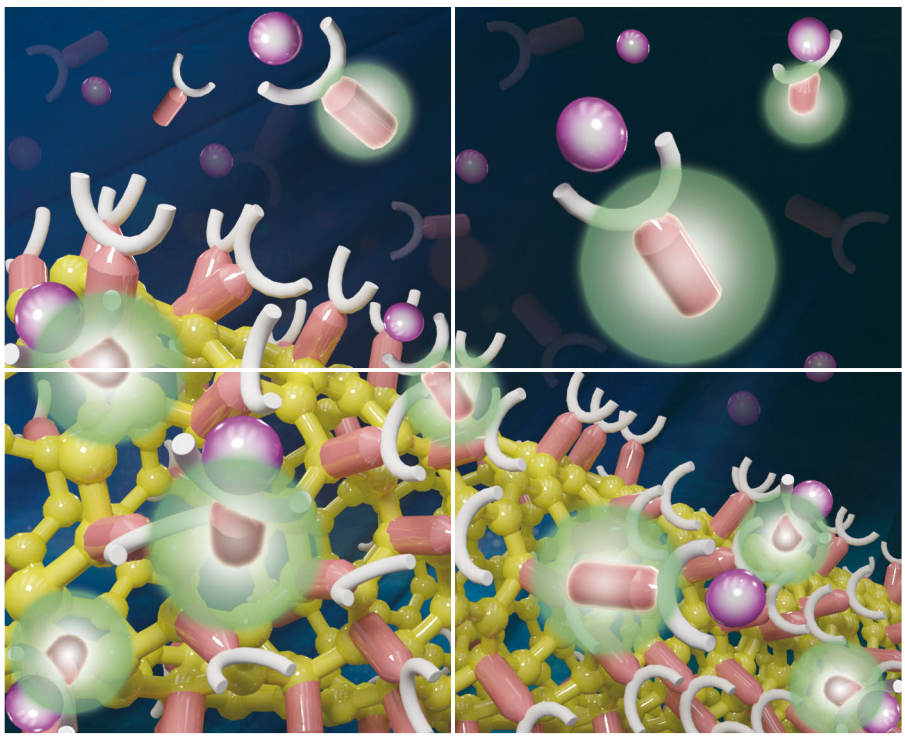

MATERIALS CHEMISTRY

FRONTIERS

Chinese Chemical Society

ROYAL SOCIETY OF CHEMISTRY

http://rsc.li/frontiers-materials

MATERIALS CHEMISTRY
FRONTIERS

RESEARCH ARTICLE

View Article Online
View Journal | View Issue

Cite this: *Mater. Chem. Front.*, 2017, **1**, 61

Received 3rd August 2016,
Accepted 4th October 2016

DOI: 10.1039/c6qm00158k

rsc.li/frontiers-materials

Low-dimensional materials facilitate the conjugation between fluorogenic boronic acids and saccharides†

Shi Guo,‡[a] Jie Chen,‡[a] Bi-Ying Cai,[a] Wen-Wen Chen,[a] Yu-Fei Li,[a] Xiaolong Sun,[b] Guo-Rong Chen,[a] Xiao-Peng He*[a] and Tony D. James*[c]

Here we demonstrate that low-dimensional materials (LDMs) enhance the conjugation between fluorogenic boronic acids (BAs) and saccharides. Among the LDMs investigated, 1D carbon nanotubes significantly lower the limit of detection and enhance the binding of the BA with D-fructose.

The development of synthetic receptors capable of imitating the active sites of natural biological receptors are of particular interest in the advancement of sensor development.[1–6] Fluorophore-tagged boronic acids (fluorogenic BAs) are artificial receptors that are synthesized extensively for sensing biologically important diols such as saccharides, glyco/glycated proteins and dopamine by fluorescence and electrochemical techniques.[7–11] In addition, many other types of BAs have been developed for building polymeric materials, separation systems and imaging probes.[9–11] However, due to the moderate affinity in forming cyclic boronate esters with diols, the sensitivity of BAs for complex saccharides remains unsatisfactory.

With the rapid advancement of materials science and technology, a number of new functional materials have been produced over the past few decades. Among them the low-dimensional materials (LDMs) including the one-dimensional (1D) carbon nanotube (CNT), the 2D graphene and 2D graphene analogues have been the most attractive because of their exceptional optical, electronic and mechanical properties. Recently there has been an emerging trend to employ these LDMs (especially graphene oxide [GO] with good water solubility and biocompatibility) for biomedical applications.[12–19] While, graphene analogues such as 2D transition metal dichalcogenides and oxides have also been shown to be useful in the construction of biosensors, drug delivering platforms and theranostic materials.[12–19] We have shown in a recent study the possibility of constructing a BA/GO composite material for sensing saccharides.[20] Here we demonstrate that the presence of a proper amount of LDMs can enhance fluorogenic BA–saccharide conjugation.

Two fluorophore-tagged phenylboronic acids (**BA1**[20] and **BA2**) were synthesized (Fig. 1). We employed typical donor–π–acceptor (D–π–A)[21] chromophores, 1,8-naphthalimide and dicyanomethylene-4*H*-pyran (DCM), to couple with BA for the construction of the fluorogenic probes (Scheme S1, ESI†).[22,23] Herein, we demonstrate

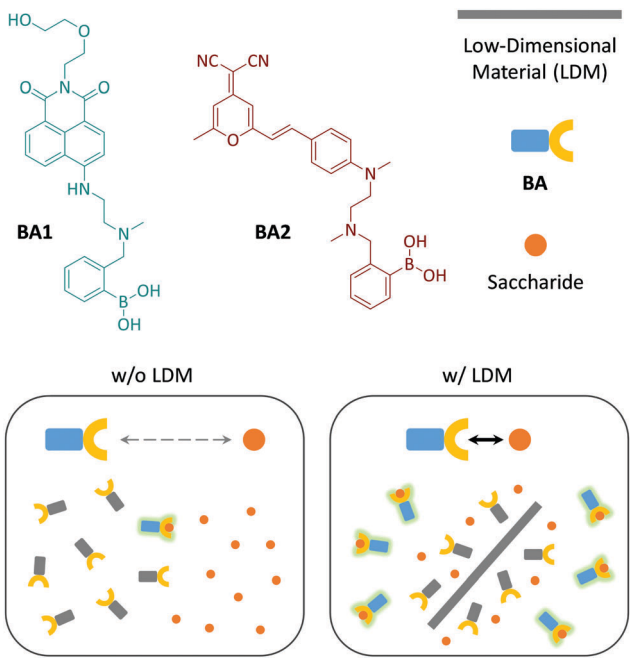

Fig. 1 Structures of the fluorogenic boronic acids (**BA1** and **BA2**) used in this study and schematic illustration of the low-dimensional material (LDM) enhanced conjugation between BA and saccharides.

[a] *Key Laboratory for Advanced Materials & Institute of Fine Chemicals, School of Chemistry and Molecular Engineering, East China University of Science and Technology, 130 Meilong Rd., Shanghai 200237, P. R. China. E-mail: xphe@ecust.edu.cn*
[b] *Department of Chemistry and Biochemistry, The University of Texas at Austin, Austin, Texas 78712, USA*
[c] *Department of Chemistry, University of Bath, Bath, BA2 7AY, UK. E-mail: T.D.James@bath.ac.uk*

† Electronic supplementary information (ESI) available: Additional figures, experimental section and original spectral copies. See DOI: 10.1039/c6qm00158k
‡ Equal contribution.

that the fluorescence emission produced as a result of the BA–saccharide conjugation is enhanced in the presence of a small amount of LDMs including: 1D CNT, 2D GO, 2D molybdenum disulphide (MoS_2) and 2D manganese dioxide (MnO_2).

The carbon materials (single-walled CNT and GO) were purchased and the 2D MoS_2[24] and 2D MnO_2[25] prepared according to previous reports. The LDMs were characterized using transmission electron microscopy (TEM), dynamic light scattering (DLS), Raman spectroscopy and UV-vis spectroscopy. While tube-like objects were observed for CNT, GO appeared to be flakes of atomic-thickness (Fig. 2a). Meanwhile, thin-layer sheets were observed for 2D MoS_2 and 2D MnO_2 (Fig. 2a), and the morphology is in agreement with those observed in previous reports.[24,25] DLS indicates that 2D GO and 2D MoS_2 have a similar size distribution, whereas the particle size of 1D CNT was larger and that of 2D MnO_2, and was slightly smaller than GO (Fig. 2b).

While typical absorbance peaks were observed for the LDMs (272 nm for 1D CNT,[26] 230 nm for GO,[27] 687/617 nm for 2D MoS_2,[24] and 370 nm for 2D MnO_2[25]) (Fig. S1, ESI†), Raman spectroscopy also suggests the formation of the LDMs (Fig. S2, ESI†). For example, in-plane stretching of sp^2-carbon atoms (G band) were observed for the LDM carbon materials (1593 cm^{-1} for CNT and 1604 cm^{-1} for GO).[28] The $E1_{2g}$ and A_{1g} vibration modes corresponded to the in-plane (382.6 cm^{-1}) and out-of-plane (406.6 cm^{-1}) vibrations of Mo and S atoms, proving the formation of thin-layer MoS_2 sheets.[29] In addition, a specific fingerprint of the Mn–O vibration in the MnO_2 framework was observed at 572 cm^{-1}.[30]

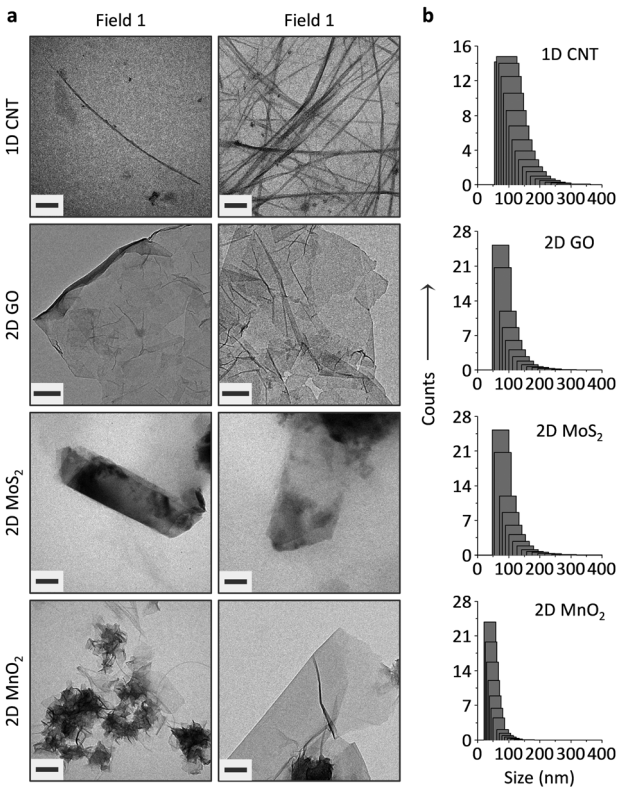

Fig. 2 (a) Transmission electron microscopy (scale bar: 200 nm) and (b) dynamic light scattering of low-dimensional materials including 1D carbon nanotube (CNT, 0.5 μg mL^{-1}), 2D graphene oxide (GO, 3 μg mL^{-1}), molybdenum disulphide (MoS_2, 0.45 μg mL^{-1}) and manganese dioxide (MnO_2, 2 μg mL^{-1}).

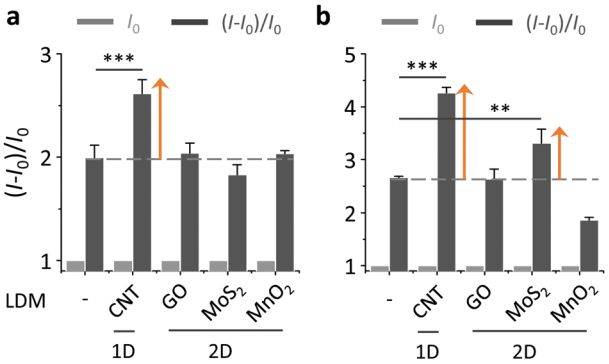

Fig. 3 Fluorescence enhancement of (a) **BA1** (20 μM) and (b) **BA2** (20 μM) with D-fructose (30 mM) in the absence (–) and presence of a low-dimensional material (LDM) including carbon nanotube (CNT, 1.25 and 0.8 μg mL^{-1} for **BA1** and **BA2**, respectively), graphene oxide (GO, 0.625 and 0.6 μg mL^{-1} for **BA1** and **BA2**, respectively), molybdenum disulphide (MoS_2, 2.5 and 10 μg mL^{-1} for **BA1** and **BA2**, respectively) and manganese dioxide (MnO_2, 2.5 and 2.0 μg mL^{-1} for **BA1** and **BA2**, respectively) in Tris-HCl (0.01 M, pH 7.4) (***$P < 0.001$; **$P < 0.05$; two-tail P values were calculated by GraphPad software). Excitation wavelength: 450 and 470 nm for **BA1** and **BA2**, respectively.

With the LDMs prepared, we then evaluated their ability to enhance the BA–saccharide conjugation (Fig. 3). As expected, we first determined that the fluorescence of both **BA1** and **BA2** increased in a concentration-dependent manner with D-fructose (fru) in a Tris-HCl buffer (Fig. S3, ESI†).[20] A blue shift was observed for **BA2** after conjugation with D-fructose. DCM has a typical D–π–A structure with a broad absorbance band because of an intramolecular charge transfer (ICT) process, therefore saccharide conjugation could compromise the planarity due to enlarged steric demand, resulting in a blue-shifted emission spectrum.[21] Subsequently, with their initial fluorescence (I_0) normalized, we tested the fluorescence enhancement [$(I - I_0)/I_0$, where I is the fluorescence intensity after conjugation with fru] of the BAs with or without LDMs. Interestingly, we determined that the presence of 1D CNT rather than other 2D LDMs led to an additional fluorescence enhancement of **BA1** with fru (with respect to **BA1** with fru alone) (Fig. 3a). In contrast, the additional fluorescence enhancement was produced by both 1D CNT and 2D MoS_2 for the conjugation between **BA2** and fru (Fig. 3b).

Subsequently, we investigated the effect of loading concentration with LDMs towards the BA–fructose conjugates. We calculated the limit of detection (LOD) for the fluorogenic BAs with D-fructose ($3\sigma/k$). The LODs of **BA1** and **BA2** in the absence and presence of the different LDMs are shown in Fig. 4. With low concentrations of CNT the LOD of **BA1** for D-fructose was lowered (which means an improved sensitivity). Likewise the LOD of **BA2** for D-fructose could also be lowered when using low concentrations of CNT and 2D MoS_2. However, a further increase of the material loading reduces the sensitivity. According to our previous study,[20a] we also determined that the fluorescence of both BAs decreased in a concentration-dependent manner with the LDMs and that the quenched

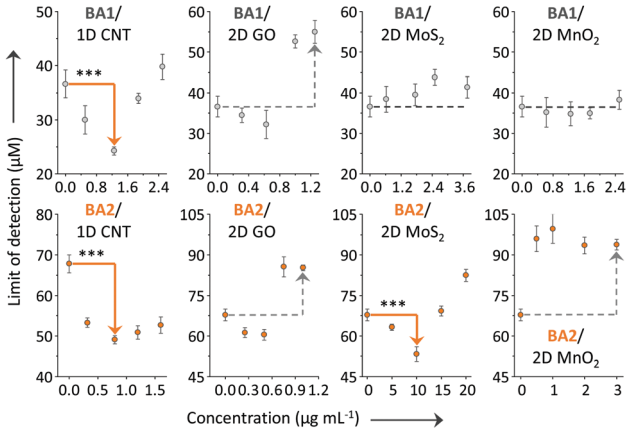

Fig. 4 Limit of detection (LOD) of **BA1** (20 μM) and **BA2** (20 μM) for D-fructose in the absence and presence of a low-dimensional material (LDM) including carbon nanotube (CNT, 0–2.5 and 0–1.6 μg mL^{-1} for **BA1** and **BA2**, respectively), graphene oxide (GO, 0–1.25 and 0–1 μg mL^{-1} for **BA1** and **BA2**, respectively), molybdenum disulphide (MoS_2, 0–3.75 and 0–20 μg mL^{-1} for **BA1** and **BA2**, respectively) and manganese dioxide (MnO_2, 0–2.5 and 0–3 μg mL^{-1} for **BA1** and **BA2**, respectively) in Tris-HCl (0.01 M, pH 7.4) (***$P < 0.001$; two-tail P values were calculated by GraphPad software). For original plots for LOD calculation, see Fig. S4–S7 (ESI†). Excitation wavelength: 450 and 470 nm for **BA1** and **BA2**, respectively.

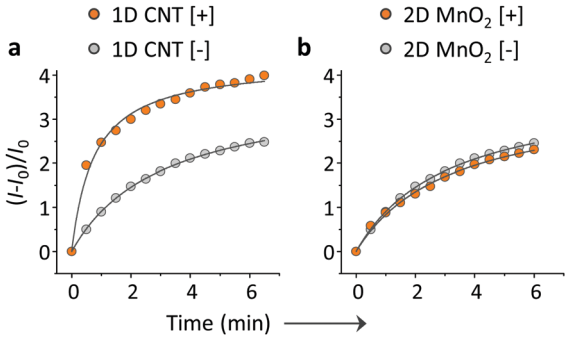

Fig. 5 Plotting the fluorescence enhancement of **BA2** (20 μM) with D-fructose (40 mM) in the absence and presence of (a) carbon nanotube (CNT, 1 μg mL^{-1}) and (b) (MnO_2, 1.25 μg mL^{-1}) as a function of time in Tris-HCl (0.01 M, pH 7.4). Excitation wavelength: 470 nm.

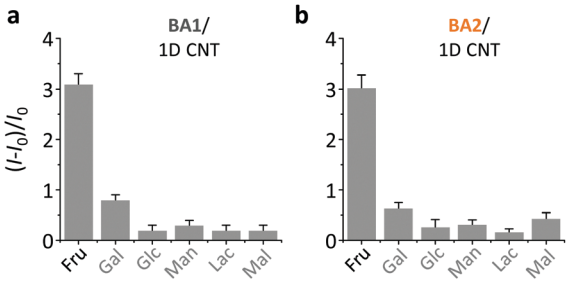

Fig. 6 Fluorescence enhancement of (a) **BA1** (20 μM) with carbon nanotube (CNT, 1.25 μg mL^{-1}) and (b) **BA2** (20 μM) with carbon nanotube (CNT, 1 μg mL^{-1}) in the presence of different saccharides (Fru = D-fructose; Gal = D-galactose; Glc = D-glucose; Man = D-mannose; Lac = D-lactose; Mal = D-maltose) (30 mM) in Tris-HCl (0.01 M, pH 7.4). Excitation wavelength: 450 and 470 nm for **BA1** and **BA2**, respectively.

fluorescence of the BA/LDM composites could be recovered gradually with increasing fru (data not shown). This precludes the possibility that the fluorescence enhancement was a result of the interaction between BA probes and LDMs alone. We have observed a similar behaviour previously, where a low concentration of GO could improve the binding between a fluorophore-tagged ligand and a protein receptor.[31,32] Low-concentration GO[33] and 2D graphene analogues[34] have also been shown to enhance the aggregation-induced-emission (AIE) of different AIEgens.

On the basis of the previous reports and data collected here we propose that the LDMs might serve as a platform to cluster both the fluorogenic BA probes and saccharides, and the approaching BA and saccharide molecules show an enhanced conjugation (Fig. 1). This has been further corroborated by a kinetic experiment that the presence of 1D CNT (Fig. 5a) rather than 2D MnO_2 (Fig. 5b) evidently accelerated the binding between **BA2** and D-fructose over a short time period. The ratio of the reaction rate constant of **BA2** in the presence of CNT to that in the absence of CNT was determined to be 3.4. Additionally, both **BA1** (Fig. 6a) and **BA2** (Fig. 6b) showed good selectivity for D-fructose over a range of other saccharides in the presence of CNT, suggesting that the sensing performance of BA is not compromised in the presence of the LDM. However, a further increase of the materials might enhance the adsorption of the fluorophores to the material surface, thus leading to fluorescence quenching, since LDMs are typically quenching materials for fluorophores.[16,17] Therefore, the smaller fluorescence enhancement of **BA1** than **BA2** with CNT (Fig. 3) might be a result of a stronger binding affinity of the former (0.79 L g^{-1}) with the material than the latter (0.18 L g^{-1}), leading to a stronger fluorescence quenching of the former. We are following up on these preliminary observations with more detailed investigations in order to probe the exact mechanism by which LDMs enhance the conjugation between the BA and saccharides and other diols.

To conclude, we have demonstrated, for the first time that BA–saccharide conjugation can be improved by LDMs when loaded at an appropriate concentration. This unique feature of LDMs enables the development of other types of BA/LDM composite materials with enhanced diol binding properties for a wide range of biomedical applications.

This research is supported by the 973 project (2013CB733700), the Science and Technology Commission of Shanghai Municipality (15540723800), the National Natural Science Foundation of China (21572058) and the Shanghai Rising-Star Program (16QA1401400). The Catalysis And Sensing for our Environment (CASE) network is thanked for research exchange opportunities. TDJ thanks ECUST for a guest professorship.

Notes and references

1 E. Galbraith and T. D. James, *Chem. Soc. Rev.*, 2010, **39**, 3831–3842.
2 T. J. Mooibroek, J. M. Casas-Solvas, R. L. Harniman, C. M. Renney, T. S. Carter, M. P. Crump and A. P. Davis, *Nat. Chem.*, 2016, **8**, 69–74.

3 H. Li, H. Valkenier, L. W. Judd, P. B. Brotherhood, S. Hussain, J. A. Cooper, O. Jurček, H. A. Sparkes, D. N. Sheppard and A. P. Davis, *Nat. Chem.*, 2016, **8**, 24–32.
4 C. Ke, H. Destecroix, M. P. Crump and A. P. Davis, *Nat. Chem.*, 2012, **4**, 718–723.
5 S.-K. Ko, S. K. Kim, A. Share, V. M. Lynch, J. Park, W. Namkung, W. V. Rosson, N. Busschaert, P. A. Gale, J. L. Sessler and I. Shin, *Nat. Chem.*, 2014, **6**, 885–892.
6 N. Busschaert, L. E. Karagiannidis, M. Wenzel, C. J. E. Haynes, N. J. Wells, P. G. Young, D. Makuc, J. Plavec, K. A. Jolliffe and P. A. Gale, *Chem. Sci.*, 2014, **5**, 1118–1127.
7 S. D. Bull, M. G. Davidson, J. M. H. van den Elsen, J. S. Fossey, A. T. A. Jenkins, Y.-B. Jiang, Y. Kubo, F. Marken, K. Sakurai, J. Zhao and T. D. James, *Acc. Chem. Res.*, 2013, **46**, 312–326.
8 X. Wu, Z. Li, X.-X. Chen, J. S. Fossey, T. D. James and Y.-B. Jiang, *Chem. Soc. Rev.*, 2013, **42**, 8032–8048.
9 M. Li, W. Zhu, F. Marken and T. D. James, *Chem. Commun.*, 2015, **51**, 14562–14573.
10 X. Sun, W. Zhai, J. S. Fossey and T. D. James, *Chem. Commun.*, 2016, **52**, 3456–3469.
11 X. Sun and T. D. James, *Chem. Rev.*, 2015, **115**, 8001–8037.
12 M. Pumera and A. H. Loo, *Trends Anal. Chem.*, 2014, **61**, 49–53.
13 Y. Chen, C. Tan, H. Zhang and L. Wang, *Chem. Soc. Rev.*, 2015, **44**, 2681–2701.
14 D. Chimene, D. L. Alge and A. K. Gaharwar, *Adv. Mater.*, 2015, **27**, 7261–7284.
15 Y. Zhang, B. Zheng, C. Zhu, X. Zhang, C. Tan, H. Li, B. Chen, J. Yang, J. Chen, Y. Huang, L. Wang and H. Zhang, *Adv. Mater.*, 2015, **27**, 935–939.
16 X.-P. He, Y. Zang, T. D. James, J. Li and G.-R. Chen, *Chem. Soc. Rev.*, 2015, **44**, 4239–4248.
17 X.-P. He and H. Tian, *Small*, 2016, **12**, 144–160.
18 C. Zhu, Z. Zeng, H. Li, F. Li, C. Fan and H. Zhang, *J. Am. Chem. Soc.*, 2013, **135**, 5998–6001.
19 H. Fan, Z. Zhao, G. Yan, X. Zhang, C. Yang, H. Meng, Z. Chen, H. Liu and W. Tan, *Angew. Chem., Int. Ed.*, 2015, **54**, 4801–4805.
20 (*a*) X. Sun, B. Zhu, D.-K. Ji, Q. Chen, X.-P. He, G.-R. Chen and T. D. James, *ACS Appl. Mater. Interfaces*, 2014, **6**, 10078–10082; (*b*) X. Sun, Q. Xu, G. Kim, S. E. Flower, J. P. Lowe, J. Yoon, J. S. Fossey, X. Qian, S. D. Bull and T. D. James, *Chem. Sci.*, 2014, **5**, 3368–3373.
21 H. Zhu, B. Liu, J. Liu, W. Zhang and W.-H. Zhu, *J. Mater. Chem. C*, 2015, **3**, 6882–6890.
22 S. Banerjee, J. A. Kitchen, S. A. Bright, J. E. O'Brien, D. C. Williams, J. M. Kelly and T. Gunnlaugsson, *Chem. Commun.*, 2013, **49**, 8522–8524.
23 R. B. P. Elmes, M. Erby, S. A. Bright, D. C. Williams and T. Gunnlaugsson, *Chem. Commun.*, 2012, **48**, 2588–2590.
24 U. Halim, C. R. Zheng, Y. Chen, Z. Lin, S. Jiang, R. Cheng, Y. Huang and X. Duan, *Nat. Commun.*, 2013, **4**, 2213.
25 D. He, X. Yang, X. He, K. Wang, X. Yang, X. He and Z. Zou, *Chem. Commun.*, 2015, **51**, 14764–14767.
26 A. G. Ryabenko, T. V. Dorofeeva and G. I. Zvereva, *Carbon*, 2004, **42**, 1523–1535.
27 D. Li, M. B. Müller, S. Gilje, R. B. Kaner and G. G. Wallace, *Nat. Nanotechnol.*, 2008, **3**, 101–105.
28 Z. Ni, Y. Wang, T. Yu and Z. Shen, *Nano Res.*, 2008, **1**, 273–291.
29 C. Lee, H. Yan, L. E. Brus, T. F. Heinz, J. Hone and S. Ryu, *ACS Nano*, 2010, **4**, 2695–2700.
30 C. Julien, M. Massot, R. Baddour-Hadjean, S. Franger, S. Bach and J. P. Pereira-Ramos, *Solid State Ionics*, 2003, **159**, 345–356.
31 D.-K. Ji, Y. Zhang, X.-P. He and G.-R. Chen, *J. Mater. Chem. B*, 2015, **3**, 6656–6661.
32 D.-K. Ji, Y. Zhang, Y. Zang, W. Liu, X. Zhang, J. Li, G.-R. Chen, T. D. James and X.-P. He, *J. Mater. Chem. B*, 2015, **3**, 9182–9185.
33 X. Qi, H. Li, J. W. Y. Lam, X. Yuan, J. Wei, B. Z. Tang and H. Zhang, *Adv. Mater.*, 2012, **24**, 4191–4195.
34 C. Tan, X. Qi, X. Huang, J. Yang, B. Zheng, Z. An, R. Chen, J. Wei, B. Z. Tang, W. Huang and H. Zhang, *Adv. Mater.*, 2014, **24**, 1735–1739.

